N-*tert*-Butylanilino Radicals. 3. X-Ray Crystallographic Structure Determination of 1,4-Di-*tert*-butyl-1,4-diaryl-2-tetrazenes and a Single-Crystal Electron Spin Resonance Study of *N*-*tert*-Butylanilino Radical Pairs

S. F. Nelsen,* R. T. Landis II, and J. C. Calabrese

Department of Chemistry, University of Wisconsin, Madison, Wisconsin 53706

Received March 25, 1977

The structures, determined by x-ray crystallography, are reported for 1,4-di-*tert*-butyl-1,4-bis(4-chlorophenyl)-2-tetrazene (**2A**) and 1,4-di-*tert*-butyl-1,4-bis(2,4,6-trideuteriophenyl)-2-tetrazene (**2B**). Crystals of **2A** are triclinic, $P\bar{1}$, with a = 8.654 (3), b = 6.648 (1), c = 9.666 (2) Å, α = 86.34 (1), β = 104.15 (2), γ = 98.60 (2)°, V = 533.1 (2) Å^3, and Z = 1. The structure was solved by heavy-atom methods, and refined to R_1 = 4.9 and R_2 = 5.2% for 847 independent observed reflections. Crystals of **2B** are monoclinic, $P2_1/n$, with a = 10.7082 (6), b = 8.697 (1), c = 11.479 (1) Å, α = 90.0, β = 109.647 (9), γ = 90.0°, V = 1006.8 (2) Å^3, Z = 2. The structure was solved by direct methods, and refined to R_1 = 4.3, R_2 = 6.5% for 1118 independent observed reflections. An ESR study of triplet radical pairs formed by photolysis of **2B** determined D = −0.0110, E = 0.0004 cm^{-1}. Nitrogen hyperfine splittings were observed in some orientations, but not analyzed.

From studies of the effect of aromatic ring substituents on the thermal decomposition rates of aralkyltetrazenes **1**[2] and **2**,[1,3] we concluded that the sensitivity of the decomposition

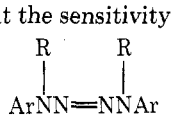

1, R = CH_3

2, R = $(CH_3)_3$

rate of **1** to substituent [rate ratio for **1** (4-OCH_3)/**1** (4-CO_2Et) of about 200 at 110 °C] was principally a conformational effect. We suggested that **1** exists in a conformation in which nitrogen lone pair, aromatic π-cloud overlap is maximized (i), but that the transition state for decomposition resembles ii,

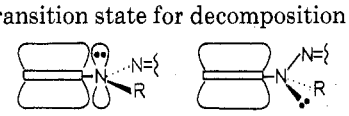

i ii

such that the breaking N–N bond is positioned for maximum delocalization of the odd electron in the anilino radical being formed.[2] The substituent effect on the rate for **1** decomposition, we proposed, largely reflects the ease of deconjugation of the nitrogen lone pair from the aromatic π system. The rate of decomposition of **2** is far less sensitive to substituent[1] (relative rates for **2** (4-OCH_3)/**2** (4-H)/**2** (4-CN) 4.5:1:1.1 at 90 °C), which we postulated was caused by the steric bulk of the *tert*-butyl group forcing **2** to assume conformation ii, in which the nitrogen lone pair is not strongly interacting with the aromatic ring.

We report here the solid-state structures of two *N*-*tert*-butylaryltetrazenes, **2A** and **2B**, and a brief ESR study of the triplet radical pairs produced by photolysis of **2B**.

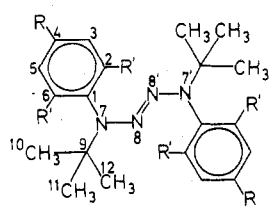

2A R=Cl, R'=H

2B R=R'=D

Experimental Section

Single-Crystal X-Ray Structure of 1,4-Di-*tert*-butyl-1,4-bis(4-chlorophenyl)-2-tetrazene (2A). A parallelepiped-shaped crystal (0.10 × 0.14 × 0.24 mm) prepared by the published method[3] and grown from pentane was attached to a glass fiber with Elmer's Glue. Preliminary oscillation, Weissenberg, and precession photographs indicated the crystal symmetry to be triclinic. The crystal was mounted on a Syntex $P\bar{1}$ four-circle computer-controlled diffractometer. Graphite-monochromated Cu Kα (λ 1.5418 Å) radiation was used throughout the alignment and data collection procedure. Lattice constants were obtained from 15 diffraction maxima well distributed in 2θ, χ, and ω. The Syntex routines[4] indicated a triclinic unit cell, with the cell parameters listed in Table I. Data were collected in the usual θ–2θ scan mode from 5° ≤ 2θ ≤ 100°. Two standard reflections monitored every 50 reflections indicated no significant drift in intensity. The data were corrected for Lorentz polarization effects with the polarization term including a correction for the graphite monochromator.[5] Absorption corrections were not applied because of the symmetrical shape of the crystal and the small value of the linear absorption coefficient.[6] The data were reduced in the usual manner[7] with $\sigma(F)$, including a term of 0.0025$(I)^2$ to avoid overweighting the strong reflections in least squares. Of the 1183 total independent measurements, the 847 with $I > 2\sigma(I)$ were used in the structural analysis.[8]

The structure was solved by the heavy-atom method.[9] The orientation of eight atoms of the *p*-chloroanilino fragment was observed as intramolecular Cl–C and Cl–N vectors comprising the three-dimensional Patterson function. Those eight atoms were included in a structure factor Fourier calculation[10] assuming the acentric space group $P1$, which then yielded the orientation of the other Cl and 17 nonhydrogen atoms. Since derived coordinates appeared to possess $\bar{1}$ site symmetry, the position of the molecule was shifted to place this point (midway between the nitrogens comprising the azo linkage) in coincidence with the center of symmetry at the origin (0,0,0). Refinement was then begun assuming the centric space group $P\bar{1}$. Nine cycles of full-matrix least-squares refinement,[11] ultimately including anisotropic temperature factors for all nonhydrogen atoms and idealized positions for hydrogen atoms using C–H distances set to 0.95 Å and B_{iso} = 5.0 Å yielded R_1 and R_2[12] of 4.9 and 5.2%. The atomic scattering factors for nonhydrogen atoms are those compiled by Hanson and co-workers,[13] and those for hydrogen atoms from Stewart and co-workers.[14] Interatomic distances and bond angles were calculated with the Busing–Martin–Levy function and error program.[15]

Aniline-*2,4,6-d*$_3$. A mixture of 31 g (0.33 mol) of freshly distilled aniline, 5 g of concentrated sulfuric acid, and 25 mL (0.13 mol) of D_2O (99.8%) was heated for 36 h at 100 °C, and then contaminated heavy water was distilled from the mixture at 1 mm. After three repetitions with 25 mL of fresh D_2O, the product was added to an ice-cold sodium carbonate solution, extracted into ether, dried with sodium sulfate, and distilled, giving aniline-d_3 appearing to have about 98% incorporation of three deuteriums by NMR: ^{1}H NMR (CCl_4) δ 6.96 (s, 2 H), 3.1 (br s, 2 H).

1,4-Di-*tert*-butyl-1,4-bis(2,4,6-trideuteriophenyl)-2-tetrazene (2B). The deuterated aniline was *tert*-butylated in methylene chloride by the method employed for the protio material[3] in 90% yield, bp 42 °C (0.45 mm). Nitrosation, reduction to the hydrazine, and

Table I. Unit Cell Parameters of 2A and 2B

	2A	2B
a, Å	8.654 (3)	10.7082 (6)
b, Å	6.648 (1)	8.697 (1)
c, Å	9.666 (2)	11.479 (1)
α, deg	86.34 (1)	90.0
β, deg	104.15 (2)	109.647 (9)
γ, deg	98.60 (2)	90.0
Volume, Å^3	533.1 (2)	1006.8 (2)
Density (calcd), g cm^{-3}	1.22	1.01
Density (obsd), g cm^{-3}	1.12	1.02
Mol/cell	1	2
Space group symmetry	$P\bar{1}$	$P2_1/n$

quinone oxidation[3] gave the tetrazene, mp 114.5–115 °C dec. Spectral data: ^{1}H NMR ($CDCl_3$) δ 7.27 (s, 4 H), 1.02 (s, 18 H); UV (EtOH) 297 (6200), 238 (9900) nm.

Single-Crystal X-Ray Structure of 1,4-Di-*tert*-butyl-1,4-bis(2,4,6-trideuteriophenyl)-2-tetrazene (2B). A single crystal of **2B** of appropriate size was cut from a large single crystal grown by slow evaporation from pentane; this compound tends to crystallize in leaves. Alignment and obtainment of cell parameters were performed as for **2A.** The Syntex autoindexing procedure indicated a monoclinic unit cell. Data were collected from $5° \leq 2\theta \leq 110°$. Standard reflection intensity data indicated no significant drift in intensity. Nine reflections exceeded the rate limits of the x-ray counter and were manually scaled to fit the remaining data by comparison with several other reflections. The data were reduced as described for **2A** to yield 1118 independent reflections significantly above background [$I > 2\sigma(I)$], which were used in the solution and refinement of the structure. Inspection of systematic absences in the merged data confirmed the choice of space group as $P2_1/n$. Since the observed density indicated the presence of two molecules per cell, this required that the molecules lie on the inversion center.

Solution of the structure was completed by direct methods. The independent data were first converted to the normalized structure factors (E values) by the program FAME.[16] The program MULTAN then generated 16 sets of possible solutions by the symbolic addition method, two of which indicated significantly greater phase angle consistency than the others. One of these gave a Fourier map which could not be interpreted in terms of a meaningful physical structure, but the second solution allowed recognition of all 12 nonhydrogen atoms. After several cycles of full-matrix isotropic least-squares refinement, idealized positions of the hydrogen atoms were included in fixed atom contributions based on C–H bond distances of 1.0 Å and $B_0 = 4.0$ Å^2, and the values of R_1 and R_2 converged to 13.6 and 22.0%, respectively. The 12 nonhydrogen atoms were then allowed anisotropic thermal motion and R_1 dropped to 5.2%. A Fourier difference map based on the 12 nonhydrogen atoms then revealed the true positions of all 14 hydrogen atoms, and these coordinates were allowed to refine isotropically in the full-matrix procedure, yielding final values of R_1 and R_2 of 4.3 and 6.5%.

ESR spectra were determined using a Varian E.3 spectrometer. A crystal of **2B** was attached with silicone grease to the horizontal face of a brass cylinder with a horizontal cut to the axis and a vertical cut along the axis. The brass fitting was then attached to a stainless steel rod which extended into the ESR cavity, inside a liquid nitrogen Dewar. After cooling, irradiation, and collection of spectra, the sample was allowed to slowly return to room temperature and the crystal checked for cracks or shifts of positions, and then moved to the vertical face, where spectra were recorded with the crystal attached in two mutually perpendicular directions.

Results and Discussion

X-Ray Structure Determination. The p-chloro compound **2A** was chosen for study because of the ease of analysis by heavy-atom methods. The deuterated compound **2B** was chosen for simplification of the triplet radical pair ESR spectrum (see following section). When it was shown that, although the solid-state conformations of **2A** and **2B** were similar their crystal packing was considerably different, the refinement of **2A** was not carried out to as great a degree as that of **2B,** which was used for the ESR study. The positional and thermal parameters for **2A** and **2B** appear in Tables II and III, and the heavy-atom bond distances and bond angles in Tables IV and V. Thermal ellipsoid plots appear in Figures 1 and 2. The agreement in intramolecular structure between **2A** and **2B** is seen to be excellent, although the distortion suggested in the C–C distances of the *tert*-butyl group of **2A**

Table II. Positional and Thermal Parameters for 2A [a,b]

Atom	x	y	z	$10^4\beta_{11}$	$10^4\beta_{22}$	$10^4\beta_{33}$	$10^4\beta_{12}$	$10^4\beta_{13}$	$10^4\beta_{23}$
Cl(4)	0.2525 (2)	−0.5776 (2)	−0.3777 (2)	184 (3)	314 (5)	231 (3)	37 (3)	94 (2)	−89 (3)
C(4)	0.1361 (6)	−0.4280 (9)	−0.3145 (6)	122 (9)	249 (18)	139 (9)	24 (10)	33 (7)	−57 (10)
C(3)	0.0445 (6)	−0.5151 (8)	−0.2234 (6)	236 (12)	226 (16)	189 (11)	57 (12)	101 (10)	23 (11)
C(2)	−0.0455 (7)	−0.3957 (9)	−0.1713 (6)	233 (12)	250 (18)	149 (9)	63 (12)	111 (9)	51 (10)
C(1)	−0.0465 (6)	−0.1938 (8)	−0.2137 (5)	120 (9)	220 (16)	100 (8)	18 (10)	24 (7)	−21 (9)
C(6)	0.0455 (6)	−0.1106 (8)	−0.3074 (6)	158 (10)	210 (16)	159 (9)	17 (10)	65 (9)	3 (10)
C(5)	0.1365 (6)	−0.2292 (9)	−0.3588 (6)	159 (10)	262 (19)	159 (9)	14 (11)	82 (8)	4 (10)
N(7)	−0.1355 (5)	−0.0619 (6)	−0.1600 (5)	129 (8)	249 (13)	117 (7)	37 (8)	31 (6)	−32 (7)
N(8)	−0.0723 (4)	0.0094 (6)	−0.0238 (5)	133 (7)	209 (11)	112 (6)	19 (9)	31 (7)	−25 (7)
C(9)	−0.3155 (6)	−0.0923 (8)	−0.1975 (6)	122 (10)	302 (18)	128 (9)	32 (10)	33 (7)	−14 (10)
C(10)	−0.3694 (7)	0.1117 (11)	−0.1916 (8)	183 (12)	418 (24)	286 (14)	121 (14)	28 (11)	−60 (14)
C(11)	−0.3735 (7)	−0.1667 (10)	−0.3493 (7)	137 (11)	518 (25)	146 (10)	34 (13)	14 (8)	−31 (13)
C(12)	−0.3845 (7)	−0.2467 (11)	−0.0969 (7)	178 (12)	517 (26)	173 (11)	−23 (14)	70 (9)	−2 (13)
H(2)	0.0441	−0.6648	−0.1951	5.0[c]					
H(3)	−0.1101	−0.4550	−0.1017	5.0[c]					
H(5)	0.0384	0.0315	−0.3405	5.0[c]					
H(6)	0.2068	−0.1706	−0.4235	5.0[c]					
H(10A)	−0.2996	0.2255	−0.2346	5.0[c]					
H(10B)	−0.3603	0.1487	−0.0905	5.0[c]					
H(10C)	−0.4851	0.1201	−0.2468	5.0[c]					
H(11A)	−0.3191	−0.0793	−0.4184	5.0[c]					
H(11B)	−0.3492	−0.3109	−0.3540	5.0[c]					
H(11C)	−0.4946	−0.1711	−0.3896	5.0[c]					
H(12A)	−0.3391	−0.3786	−0.0971	5.0[c]					
H(12B)	−0.5040	−0.2756	−0.1233	5.0[c]					
H(12C)	−0.3483	−0.1946	0.0032	5.0[c]					

[a] The form of the anisotropic temperature factor which is used is $\exp[-(\beta_{11}h^2 + \beta_{22}k^2 + \beta_{33}l^2 + 2\beta_{12}hk + 2\beta_{13}hl + 2\beta_{23}kl)]$. [b] The standard deviations in the last significant figure are given in parentheses in this and succeeding tables. [c] Isotropic thermal parameters.

Table III. Positional and Thermal Parameters for 2B[a,b]

Atom	x	y	z	$10^4\beta_{11}$	$10^4\beta_{22}$	$10^4\beta_{33}$	$10^4\beta_{12}$	$10^4\beta_{13}$	$10^4\beta_{23}$
C(1)	0.2705 (1)	0.5705 (2)	0.4601 (1)	75	153	85	−1	33	15
C(2)	0.2386 (2)	0.7156 (2)	0.4883 (2)	123	165	124	12	31	1
C(3)	0.1469 (2)	0.8034 (3)	0.4007 (2)	145	186	171	38	29	24
C(4)	0.0872 (2)	0.7477 (3)	0.2850 (2)	106	220	154	13	27	70
C(5)	0.1170 (2)	0.6038 (3)	0.2544 (2)	123	279	96	−32	22	25
C(6)	0.2111 (2)	0.5140 (3)	0.3426 (2)	118	187	99	2	38	6
N(7)	0.3684 (1)	0.4851 (2)	0.5550 (1)	83	147	94	0	39	18
N(8)	0.4883 (1)	0.4551 (1)	0.5373 (1)	82	130	87	−3	34	8
C(9)	0.3280 (2)	0.3537 (2)	0.6183 (1)	106	157	90	−23	45	12
C(10)	0.3068 (4)	0.2077 (3)	0.5425 (2)	296	181	142	−93	87	−3
C(11)	0.2021 (3)	0.3997 (4)	0.6421 (3)	169	335	220	31	131	105
C(12)	0.4374 (3)	0.3283 (3)	0.7412 (2)	165	248	116	−42	27	63
D(6)	0.2377 (18)	0.4196 (23)	0.3209 (16)	5.325[c]					
H(5)	0.0809 (22)	0.5603 (23)	0.1710 (19)	6.729[c]					
D(4)	0.0261 (21)	0.8107 (22)	0.2250 (19)	6.175[c]					
H(3)	0.1193 (28)	0.9075 (34)	0.4159 (24)	10.144[c]					
D(3)	0.2819 (23)	0.7532 (24)	0.5713 (22)	7.025[c]					
H(10A)	0.2898 (24)	0.1251 (27)	0.5878 (21)	7.931[c]					
H(10B)	0.2267 (29)	0.2312 (24)	0.4630 (27)	9.317[c]					
H(10C)	0.3977 (32)	0.1835 (35)	0.5213 (27)	11.970[c]					
H(11A)	0.1244 (29)	0.4104 (33)	0.5620 (25)	9.861[c]					
H(11B)	0.2221 (39)	0.5042 (45)	0.6898 (33)	14.592[c]					
H(11C)	0.1794 (24)	0.3183 (31)	0.6893 (24)	8.712[c]					
H(12A)	0.5217 (31)	0.3122 (30)	0.7286 (25)	9.632[c]					
H(12B)	0.4392 (25)	0.4326 (30)	0.7895 (22)	9.236[c]					
H(12C)	0.4140 (20)	0.2489 (25)	0.7855 (20)	6.694[c]					

[a] The form of the anisotropic temperature factor which is used is $\exp[-(\beta_{11}h^2 + \beta_{22}k^2 + \beta_{33}l^2 + 2\beta_{12}hk + 2\beta_{13}hl + 2\beta_{23}kl)]$. [b] The standard deviations in the last significant figure are given in parentheses in this and succeeding tables. [c] Isotropic thermal parameters.

Table IV. Heavy-Atom Intramolecular Distances for 2A and 2B (Å)

	2A	2B
C(1)–C(2)	1.379 (7)	1.374 (3)
C(2)–C(3)	1.387 (8)	1.376 (3)
C(3)–C(4)	1.367 (7)	1.356 (3)
C(4)–C(5)	1.363 (7)	1.366 (3)
C(5)–C(6)	1.384 (7)	1.401 (3)
C(1)–C(6)	1.384 (7)	1.374 (3)
C(1)–N(7)	1.445 (6)	1.439 (2)
N(7)–N(8)	1.381 (5)	1.390 (2)
N(8)–N(8′)	1.246 (7)	1.246 (2)
N(7)–C(9)	1.496 (6)	1.494 (2)
C(9)–C(10)	1.507 (8)	1.513 (3)
C(9)–C(11)	1.519 (8)	1.516 (3)
C(9)–C(12)	1.527 (8)	1.516 (3)
N(7)–N(7′)	3.456 (11)	3.464 (4)
C(4)–Cl	1.748 (5)	

Table V. Heavy-Atom Bond Angles for 2A and 2B (deg)

	2A	2B
C(2)–C(1)–C(6)	119.28 (47)	119.36 (17)
C(3)–C(2)–C(1)	120.35 (50)	120.67 (20)
C(4)–C(3)–C(2)	119.05 (51)	120.21 (22)
C(5)–C(4)–C(3)	121.75 (48)	120.33 (19)
C(6)–C(5)–C(4)	119.15 (50)	119.92 (20)
C(1)–C(6)–C(5)	120.37 (50)	119.50 (20)
C(2)–C(1)–N(7)	122.55 (46)	118.10 (15)
C(6)–C(1)–N(7)	118.13 (47)	122.52 (16)
C(1)–N(7)–N(8)	117.71 (39)	117.39 (11)
N(7)–N(8)–N(8′)	113.71 (49)	113.07 (12)
C(1)–N(7)–C(9)	121.16 (41)	120.42 (12)
N(8)–N(7)–C(9)	112.09 (37)	111.12 (12)
N(7)–C(9)–C(10)	107.63 (45)	111.97 (15)
N(7)–C(9)–C(11)	108.25 (43)	107.87 (16)
N(7)–C(9)–C(12)	111.99 (46)	107.70 (14)
C(10)–C(9)–C(11)	108.90 (52)	110.76 (22)
C(11)–C(9)–C(12)	109.41 (49)	109.41 (20)
C(10)–C(9)–C(12)	110.57 (50)	109.05 (20)
C(3)–C(4)–Cl	118.93 (41)	
C(5)–C(4)–Cl	119.31 (44)	

is not borne out in the more refined structure for **2B.** The hydrogens refined to reasonable positions for **2B,** the aliphatic hydrogens giving final C–H distances of 0.940 (25)–1.101 (28) Å and the aromatic C–D distances obtained were 0.966 (22), 0.948 (21), and 0.930 (19) Å at C(2), C(4), and C(6), marginally shorter than the 0.986 (29) and 0.980 (20) Å obtained for the C(3) and C(5) C–H bonds.

The geometries found at the planar tetrazene linkages are compared in Figure 3. Some preliminary structural data have been reported for two aliphatic *trans*-2-tetrazenes, azomorpholine (**3**) and the bistetrazene 1,4,7,10-tetramethyl-1,2,3,4,7,8,9,10-octaazacyclododeca-2,8-diene (**4**),[17] which have N–N distances of 1.393 (1) and 1.385 (2, av, max dev 7) Å and N=N distances of 1.251 (2) and 1.253 (2, av, max dev 1) Å, respectively, and N—N=N angles averaging 113.0 (2, max dev 4)°; the geometry at the tetrazine linkage of **2** closely resembles that of **3** and **4.**

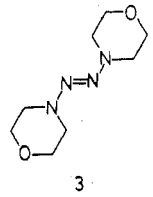

3

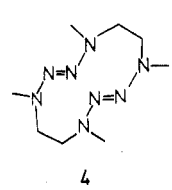

4

Information on the dihedral angles between planes containing several atoms in **2B** appears in Table VI. The aryl ring and N(7) lie in plane, and the two aryl rings of each molecule are in parallel planes, separated by 2.98 Å. The planes of the aryl rings have a dihedral angle of 57° with respect to the tetrazene nitrogen plane. The trisubstituted nitrogen is nonplanar, N(7) lying 0.28 Å from the plane through the three

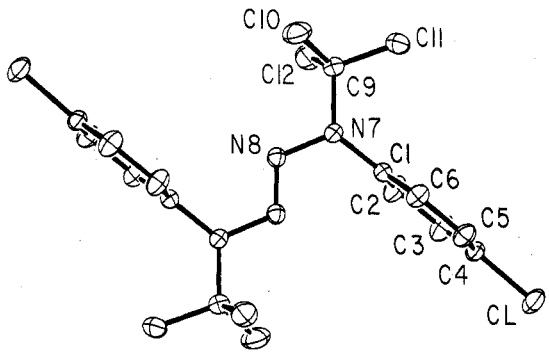

Figure 1. Thermal ellipsoid plot of **2A**, hydrogens omitted.

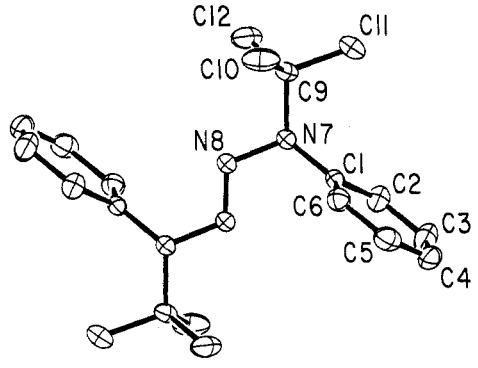

Figure 2. Thermal ellipsoid plot of **2B**, hydrogens omitted.

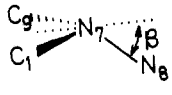

atoms attached to it [plane 4, C(1)–N(8)–C(9)], $\beta = 34.1°$. The lone pair of N(7) was not observed by x-ray analysis, but its axis should lie approximately perpendicular to plane 4. The lone-pair orbital axis is thus inferred to lie nearly in the plane of the aryl ring, so that **2** does indeed have the "deconjugated" conformation suggested previously.[1,3] The flattening at N(7) must be largely steric, because the N(7) lone pair is twisted out of conjugation with both the aryl ring and the azo linkage. For the single-crystal ESR study, the relationship between the symmetry-related molecules and the crystal faces are important. A packing diagram appears in Figure 4, and intermolecular closest heavy-atom approaches are shown in Table VII. Table VIII contains information on the relationship of the aryl ring planes in the symmetry-related pairs of molecules, and the orientation of these planes with respect to the crystal faces. The aryl rings of the two types of symmetry-related **2B** molecules within the crystal make an angle of 45° with each other, and the aryl rings are nearly perpendicular (97° angle) with the A face of the crystal.

Triplet Radical Pairs from 2. Since the pioneering study by Bartlett and McBride[18] of α-phenylethyl triplet radical pairs trapped in a matrix of the azo compound, several other triplet radical pairs have been studied. Radical precursors have included azo compounds,[18,19] tetraphenylhydrazine,[20] and diacyl peroxides;[21,22] especially detailed studies of the triplet pairs from benzoylacetyl peroxide have been carried out.[23] It was expected from this work that *N*-*tert*-butylanilino triplet radical pairs would be observed upon photolysis of **2**, as proved to be the case. When powdered samples of **2** are photolyzed at liquid nitrogen temperature, powder spectra of a triplet with D of about 100 G, as well as a weak half-field absorption, are observed. Single crystals of variously substituted **2** molecules gave strongly anisotropic ESR spectra,

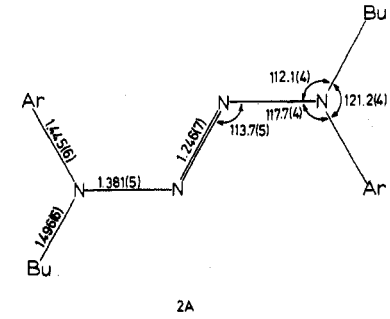

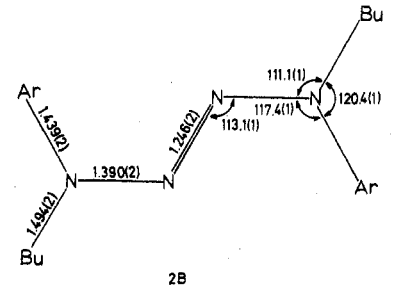

Figure 3. Comparison of geometries at the 2-tetrazene linkage for **2A** and **2B**.

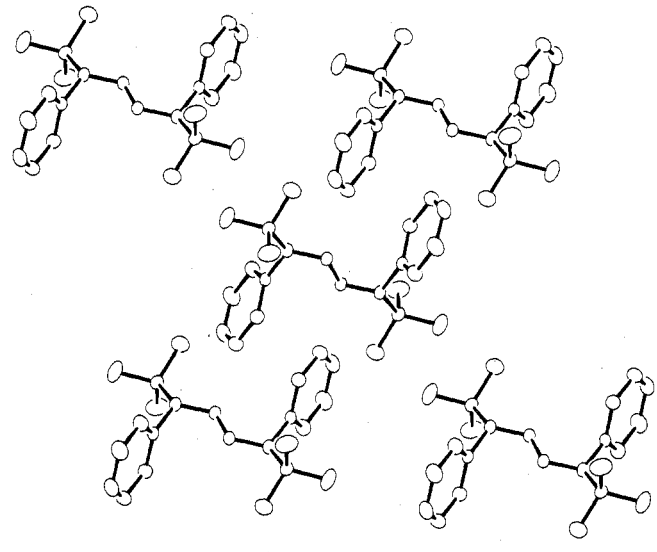

Figure 4. Packing diagram for **2B**, showing four molecules of one orientation surrounding one of the other orientations.

Table VI. Planes and Dihedral Angles in 2B

Atoms in place	Plane no.	Atoms out of plane (distance, Å)
C(1)–C(2)–C(3)–C(4)–C(5)–C(6)	1	N(7) (+0.01), N(8) (+1.15)
C(1′)–C(2′)–C(3′)–C(4′)–C(5′)–C(6′)	2	N(7′) (−0.01), N(8) (−1.15)
N(7)–N(8)–N(8′)–N(7′)	3	C(1) (+1.15), C(6) (+1.49)
C(1)–N(8)–C(9)	4	N(7) (−0.28), C(4) (+0.40)

Angles (deg) between Plane n and the Other Planes

Planes	2	3	4
1	0.01	57.16	94.18
2		57.16	94.18
3			96.19

Table VII. Intramolecular Aryl Group Closest Approaches for 2B

Atoms[a]	Distance, Å
C(2)–C(4″)	4.133 (4)
C(3)–C(6″)	4.040 (4)
C(3)–C(12″)	3.985 (4)
C(4)–C(6‴)	3.781 (3)
C(4)–N(8‴)	3.948 (4)
C(4)–N(7″)	3.701 (3)
C(4)–N(8″)	3.723 (3)

[a] The ″ designation refers to the half-molecule fragment related by the symmetry operation $\frac{1}{2} + x, \frac{1}{2} - y, \frac{1}{2} + z$, and the ‴ to the half-molecule fragment related by $\frac{1}{2} - x, \frac{1}{2} + y, \frac{1}{2} - z$.

Table VIII. Intermolecular and Crystal Face Planes in 2B

Atoms in plane	Plane no.
C(1)–C(2)–C(3)–C(4)–C(5)–C(6)	1
C(1″)–C(2″)–C(3″)–C(4″)–C(5″)–C(6″)	5
Crystal face A	6
Crystal face B	7
Crystal face C	8

Planes	Angles (deg) between Plane n and the Other Planes 5	6	7	8
1	45.47	97.04	26.69	61.34
5		61.34	26.69	97.04
6			70.40	102.37
7				70.40

which showed very complex patterns in some orientations. We concluded that hyperfine splittings were being observed in the dipolar splitting lines. The isotropic ESR spectrum of *N*-phenylanilino radical in solution shows several splittings of comparable magnitude; $a(N) = 9.70$ $a(H_p) = 7.09$, $a(2H_o) = 5.74$, $a(2H_m) = 1.99$ G, $g = 2.0033$.[3] To simplify the spectra of the triplet radical pairs, we prepared the deuterated compound **2B.** Irradiation of **2B** in pentane gave the expected *N*-*tert*-butylanilino-d_3 radical isotropic ESR spectrum, $a(N) = 9.70$, $a(2H_m) = 1.97$, $a(3D) \approx 1.0$ g, $g = 2.0033$. The isotropic nitrogen splitting is five times larger than any of the other splittings in the deuterated material. Since spectral lines attributable to less highly deuterated *N*-*tert*-butylanilino radicals were not observed, a usefully high degree of deuterium incorporation in **2B** had been achieved.

A single crystal of **2B** was mounted to a brass fitting attached to a rod which could be rotated inside a liquid nitrogen Dewar in the cavity of the ESR spectrometer. The brass fitting had faces perpendicular and parallel to the axis of rotation, so that by mounting the same face of the crystal to these faces, rotations about three mutually perpendicular axes could be achieved. ESR spectra were recorded at 10–15° rotation intervals about each of these three mutually perpendicular axes, after irradiation at liquid nitrogen temperature. In addition to a large central peak about 50 G wide, attributed to the monoradical, four peaks (which were split further in some orientations) were found to have positions very sensitive to rotation angle. Because of the two orientations of **2B** known to be present in the crystal, this is expected; loss of nitrogen from the symmetry-related tetrazene molecules should give radical pairs in two different orientations, and each radical pair will give rise to an anisotropic doublet ESR spectrum, because of its dipolar splitting. The orientation of the crystal employed (large face parallel and perpendicular to the axis of rotation) nearly coincided with the principal axes of one dipolar doublet (hereafter called species I), and the anisotropy

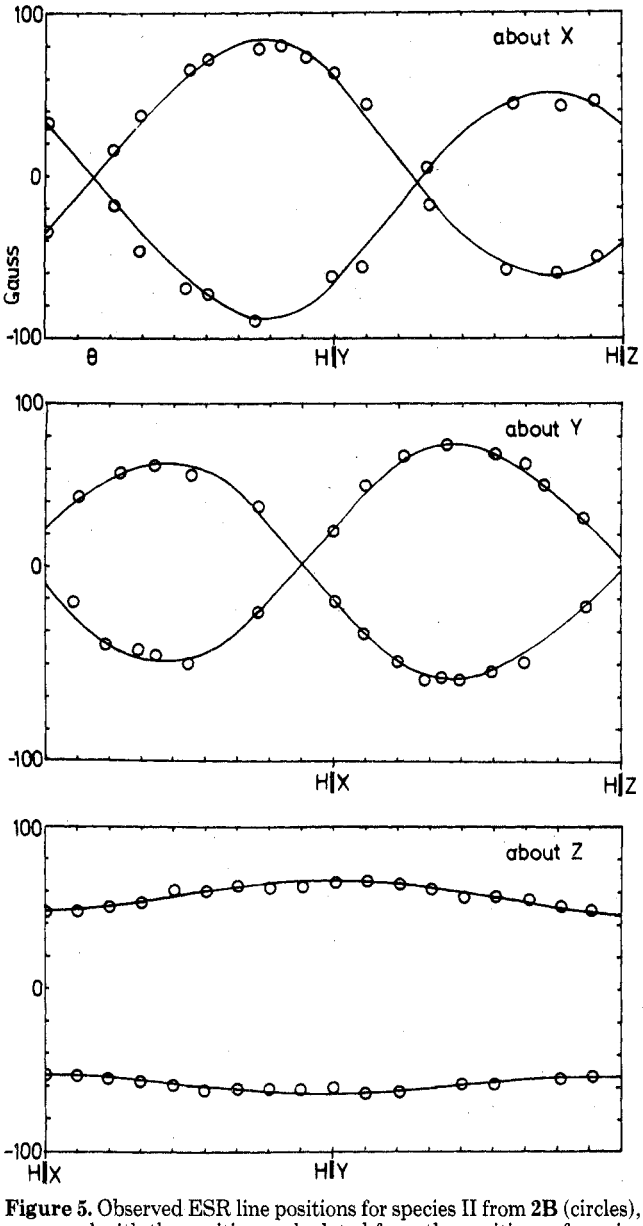

Figure 5. Observed ESR line positions for species II from **2B** (circles), compared with the positions calculated from the positions of species I and the relative orientation of the two types of **2B** molecules in the crystal (Table VIII).

of the line positions was analyzed by the method described in Wertz and Bolton,[24] giving a D matrix which was diagonalized, allowing calculation of the zero-field splitting parameters $D' = (-)117$ G, $E' = (+)4$ G ($D = (-)0.0110$, $E = (+)0.0004$ cm^{-1}). In a further check on our analysis, the line separations for species I were plotted vs. $\sin^2 \theta$, giving straight lines for which D and E can be estimated using the equations of Vincent and Maki[25] for rotation about the principal axes, giving $D' = 0.0110, 0.0108, 0.0112$, and $E' = 0.00018, 0.00065, 0.0004$, respectively, for the three axes of rotation used, in good agreement with the matrix diagonalization analysis. Species II clearly did not have its principal axes aligned in the directions for rotation chosen, as expected from the crystal structure. The expected spectrum was calculated, again using the equations of Vincent and Maki, from the relative orientation of the two molecules in the crystal lattice of **2B** (see Figure 4 for a packing diagram, and Table VIII for the relative orientation of the molecules in the crystal), resulting in fairly good agreement to the observed line positions for species II, as shown in Figure 5.

The D value for the *N*-*tert*-butylanilino radicals from **2B** corresponds to an average odd electron separation of over 5

Å. Great motion of the radicals with respect to each other upon loss of nitrogen is not expected, because of the good alignment of the C(1)–N(7) bond with the aryl π cloud in the tetrazene. Our ESR data is not good enough to measure the actual amount of motion of the radicals from their positions in the tetrazene precursor, as McBride and co-workers[19,23] have done for several crystals. As a qualitative way of gauging motion, we calculated the D' and E' expected using the spin densities estimated from the doublet ESR spectrum ($\rho_N = 0.489$, $\rho_o = 0.234$, $\rho_m = -0.080$, $\rho_p = -0.284$; these are only estimates, and ignore spin density in the *tert*-butyl group) and the atom positions of the tetrazene, obtaining $D' = -146$, $E' = 10$ G, both rather higher than the observed values.

The axes for the anisotropic g tensor coincided, with our rather wide experimental error, with those for the D tensor, and the observed values were $g_{zz} = 2.0058$, $g_{yy} = 2.0003$, $g_{xx} = 2.0044$, $g_{iso} = 2.0035$, close to the 2.0033 observed for the doublet in solution.

Hyperfine splittings caused by the nitrogen atoms were observed in some orientations of the triplet, but we have not been able to analyze them. No splittings were observed in the dipolar lines for orientation about the axis nearly coincident with the z axis of the triplet, although the line width varied from about 6.5 to 15 G, but in rotations about the other axes, each half of the doublet for species I varied from appearing as a singlet (splitting under 2 G) to appearing as a five to nine line pattern with apparent line separation of up to 12 G.

Quantitative study of these triplets was hampered by the presence of species I and II, which frequently merged with each other, disrupting our ability to accurately measure the line positions of either one. Preparation of deuterated **2A** would allow study of the nitrogen hyperfine splittings without this difficulty, but such a study has not been carried out.

Acknowledgment. We thank the donors of the Petroleum Research Fund, administered by the American Chemical Society, and the National Science Foundation for partial financial support of this research. The funds used for purchasing the diffractometer came partly from the Major Instrument Program of the NSF. We thank Professor J. M. McBride for extensive discussions and the program used for calculation of D' and E', and W. C. Hollinsed for assistance in calculations from the x-ray data.

Registry No.—**2A,** 63641-20-3; **2B,** 63641-21-4; aniline-2,4,6-d_3, 7291-08-9; aniline, 62-53-3; D_2O, 7789-20-0.

References and Notes

(1) For Part 2, see S. F. Nelsen and R. T. Landis II, *J. Am. Chem. Soc.*, **95,** 8707 (1973).
(2) S. F. Nelsen and D. H. Heath, *J. Am. Chem. Soc.*, **91,** 6452 (1969).
(3) S. F. Nelsen, R. T. Landis II, L. H. Kiehle, and T. H. Leung, *J. Am. Chem. Soc.*, **94,** 1610 (1972).
(4) R. A. Sparks, "Operations Manual, Syntex P$\bar{1}$ Diffractometer", Syntex Analytical Instruments, Cupertino, Calif., 1970.
(5) G. H. Stout and L. H. Jensen, "X-ray Structure Determination", Macmillan, New York, N.Y., 1968, p 411.
(6) "International Tables for X-ray Crystallography", Vol. I., The Kynoch Press, Birmingham, England, 1965.
(7) Cf., V. A. Uchtman and L. F. Dahl, *J. Am. Chem. Soc.*, **91,** 3756 (1969).
(8) Computer programs used for data reduction were FOBS and SORTMERGE, written ty the author (J.C.C.).
(9) A. L. Patterson, *Z. Kristallogr.*, **A90,** 517 (1935).
(10) J. C. Calabrese, "A Three-Dimensional Fourier Summation Program—Fourier", unpublished.
(11) ORFLSD, a local modification of the program by W. R. Busing, K. O. Martin, and H. A. Levy, "ORFLS, A Fortram Crystallographic Least Squares Program", Oak Ridge National Laboratory, Oak Ridge, Tenn. 1964, N, ORNL-TM-305.
(12) $R_1 = [\Sigma||F_o| - |F_c||/\Sigma|F_o|] \times 100$ and $R_2 = [\Sigma W_i||F_o| - |F_c||^2/\Sigma W_i|F_o|^2]^{1/2} \times 100$. All least-squares refinements were based on the mimimunation of $\Sigma W_i||F_o| - |F_c||^2$ with the individual weights $W_i = 1/\sigma(F_o)^2$.
(13) H. P. Hanson, F. Herman, J. D. Lea, and S. Skillman, *Acta Crystallogr.*, **17,** 1040 (1964).
(14) R. F. Stewart, E. R. Davidson, and W. T. Simpson, *J. Chem. Phys.*, **42,** 3175 (1965).
(15) W. R. Busing, K. O. Martin, and H. A. Levy, "ORFFE, A Fortram Crystallographic Function and Error Program", Oak Ridge National Laboratory, Oak Ridge, Tenn., 1964, No. ORNL-TM-306.
(16) R. B. K. Dewar and A. L. Stone, "FAME", University of Chicago, 1966.
(17) V. W. Day, D. H. Campbell, and C. J. Michejda, *J. Chem. Soc., Chem. Commun.*, 118 (1975).
(18) P. D. Partlett and J. M. McBride, *Pure Appl. Chem.*, **15,** 89 (1967).
(19) Detailed study of azoisobutyronitrile decomposition has been carried out by the group of McBride, but their ESR studies remain largely unpublished. For earlier studies of radical pairs from this compound, see A. S. Lebedev, *Dokl. Akad. Nauk. SSSR,* **171,** 378 (1966); M. C. R. Symons, *Nature-(London),* **213,** 1226 (1967).
(20) (a) D. A. Wiersma and J. Kommandeur, *Mol. Phys.*, **13,** 241 (1967); (b) D. A. Wiersma, J. H. Lichtenbott, and J. Kommandeur, *J. Chem. Phys.*, **50,** 2974 (1968).
(21) A. V. Zubkov, A. T. Koritskii, and Ya. S. Lebedev, *Dokl. Akad. Nauk. SSSR,* **180,** 1150 (1968).
(22) (a) H. C. Box, *J. Phys. Chem.*, **75,** 3426 (1971); (b) H. C. Box, E. E. Budzaski, and H. G. Freund, *J. Am. Chem. Soc.*, **92,** 5305 (1970).
(23) (a) N. J. Karch and J. M. McBride, *J. Am. Chem. Soc.*, **94,** 5092 (1972); (b) N. J. Karch, E. T. Koh, B. L. Whitsel, and J. M. McBride, *ibid.*, **97,** 6729 (1975).
(24) J. E. Wertz and J. R. Bolton, "Electron Spin Resonance", McGraw-Hill, New York, N.Y., 1972, p 125.
(25) J. S. Vincent and A. H. Maki, *J. Chem. Phys.*, **39,** 3088 (1963).

Telesubstitution and Other Transformations of Imidazo[1,2-a]- and s-Triazolo[4,3-a]pyrazines[1]

Jernej Bradač, Zdenka Furek, Daša Janežič, Stana Molan, Igor Smerkolj, Branko Stanovnik, Miha Tišler,* and Bojan Verček

Department of Chemistry, University of Ljubljana, 61000 Ljubljana, Yugoslavia

Received May 23, 1977

Imidazo[1,2-a]pyrazine is brominated to give either the 3-bromo- or the 3,5-dibromo derivative. The 6,8-dibromo compound, prepared from 2-amino-3,5-dibromopyrazine, is brominated to 3,6,8-tribromoimidazo[1,2-a]pyrazine. With sodium methylate only the bromine atom at position 8 is substituted, and from the 6,8-dibromo compound 6-bromo-8-methoxyimidazo[1,2-a]pyrazine is prepared. Quaternization of imidazo[1,2-a]pyrazine gives a mixture of the 1-methyl and 7-methyl derivatives. s-Triazolo[4,3-a]pyrazine afforded upon bromination the 5-bromo derivative. This and other 5-halo compounds reacted with nucleophiles to give either the anticipated 5-substituted derivative or at position 8 telesubstituted product, or both. Mechanistic aspects of telesubstitution are outlined.

As part of our interest in the chemistry of azolopyrazines we would like to report some new transformations of imidazo[1,2-a]- and s-triazolo[4,3-a]pyrazines.

A general method for the synthesis of imidazo[1,2-x]azines consists of the reaction between the corresponding 2-aminoazines and α-halocarbonyl compounds. In the pyrazine